Front. Environ. Sci. Eng. 2015, 9(6): 1084–1095
DOI 10.1007/s11783-015-0805-y

RESEARCH ARTICLE

Microbial electrolysis cells with biocathodes and driven by microbial fuel cells for simultaneous enhanced Co(II) and Cu(II) removal

Jingya SHEN[1], Yuliang SUN[1], Liping HUANG (✉)[1], Jinhui YANG[2]

1 Key Laboratory of Industrial Ecology and Environmental Engineering (Ministry of Education), School of Environmental Science and Technology, Dalian University of Technology, Dalian 116024, China
2 Experiment Center of Chemistry, Dalian University of Technology, Dalian 116024, China

Abstract Cobalt and copper recovery from aqueous Co (II) and Cu(II) is one critical step for cobalt and copper wastewaters treatment. Previous tests have primarily examined Cu(II) and Co(II) removal in microbial electrolysis cells (MECs) with abiotic cathodes and driven by microbial fuel cell (MFCs). However, Cu(II) and Co(II) removal rates were still slow. Here we report MECs with biocathodes and driven by MFCs where enhanced removal rates of $6.0\pm0.2\ mg\cdot L^{-1}\cdot h^{-1}$ for Cu(II) at an initial concentration of $50\ mg\cdot L^{-1}$ and $5.3\pm0.4\ mg\cdot L^{-1}\ h^{-1}$ for Co(II) at an initial $40\ mg\cdot L^{-1}$ were achieved, 1.7 times and 3.3 times as high as those in MECs with abiotic cathodes and driven by MFCs. Species of Cu(II) was reduced to pure copper on the cathodes of MFCs whereas Co(II) was removed associated with microorganisms on the cathodes of the connected MECs. Higher Cu(II) concentrations and smaller working volumes in the cathode chambers of MFCs further improved removal rates of Cu(II) (115.7 $mg\cdot L^{-1}\cdot h^{-1}$) and Co(II) ($6.4\ mg\cdot L^{-1}\cdot h^{-1}$) with concomitantly achieving hydrogen generation ($0.05\pm0.00\ mol\cdot mol^{-1}$ COD). Phylogenetic analysis on the biocathodes indicates *Proteobacteria* dominantly accounted for 67.9% of the total reads, followed by *Firmicutes* (14.0%), *Bacteroidetes* (6.1%), *Tenericutes* (2.5%), *Lentisphaerae* (1.4%), and *Synergistetes* (1.0%). This study provides a beneficial attempt to achieve simultaneous enhanced Cu(II) and Co(II) removal, and efficient Cu(II) and Co(II) wastewaters treatment without any external energy consumption.

Keywords biocathode, microbial electrolysis cell, microbial fuel cell, Cu(II) removal, Co(II) removal

Received April 5, 2015; accepted June 11, 2015

E-mail: lipinghuang@dlut.edu.cn

1 Introduction

Copper and cobalt are extensively used in microelectronic fields such as lithium ion batteries. Recovery of copper and cobalt from spent lithium ion batteries is thus one of the primary objectives in recycling of these wastes due to the shortage of natural ores and environmental considerations [1]. The newly developed bioelectrochemical systems (BESs) show promising for this recovery, where Cu(II) can be spontaneously reduced to Cu(0) on the cathodes of microbial fuel cells (MFCs) due to a favorable half cell redox potential of 0.34 (*vs.* standard hydrogen electrode, SHE) relative to that of organic matter (ca. −0.30 V for acetate, standard conditions), and Co(II) can be reduced in microbial electrolysis cells (MECs) at a more negative potential of −0.23 V (*vs.* SHE, standard conditions) [2,3]. Multiple factors including but are not limited to, initial Cu (II) and Co(II) concentrations, temperature, solution conductivity, pH and operation time affect system performance for Cu(II) and Co(II) removal. Remaining challenges are the requirement of a power source to overcome electrode overpotentials for Co(II) removal in MECs, the collection and harvest of low power densities from MFCs with Cu(II) removal for further utilization, and the improvement of Cu(II) and Co(II) removal rates in order for the practical application of BESs.

MECs driven by MFCs are effective to avoid the disadvantages of individual MFCs and MECs for metal removal, where MECs is the external resistance of MFCs and MFCs is the external power of MECs (Fig. 1) [4]. Compared to the individual MECs where an external power was required to recover metals of Cu(II), Pb(II), Cd (II), Zn(II) and/or Ni(II) [5–8], MECs driven by MFCs can achieve not only simultaneous Cu(II) and Co(II) recovery without any external energy consumption, but also in-site

utilize energy from MFCs, and thus avoid the difficulties in MFCs energy collection and storage, and the requirement of energy consumption in MECs [4,9,10]. Any factors influencing MFC performance reasonably affect performance of the connected MEC and vice versa. These bilateral effects in this complex MFC-MEC system thus create more challenges for process optimization and maintenance. Despite MECs with abiotic cathodes and driven by MFCs was feasible for compensating the disadvantages of individual MFCs and abiotic cathode MECs for Co(II) and Cu(II) removal [9,10], overpotentials for Co(II) removal in MECs was still high and thus resulted in low removal rates of Co(II) in MECs and consequent Cu (II) in the connected MFCs. Biocathodes, which use electrotrophs as catalysts to accept cathodic electrons, is promising for industrial applicable BESs due to its multiple merits such as sustainability and cost-effectivity [11–14]. Electrotrophs can decrease overpotentials and remove recalcitrant wastes, which enables the biocathodes more advantages over abiotic cathodes, particularly at a neutral pH environment. Biocathodes in MECs with Co(II) removal and driven by Cu(II)-removed MFCs is expected to decrease overpotentials for Co(II) removal on the cathodes of MECs and thus achieve both efficient Co(II) removal in MECs and consequent Cu(II) removal in the connected MFCs without any external energy consumption. Despite the explorations of either MFCs driving MECs with abiotic cathodes for hydrogen, cobalt, zinc and copper recovery [4,9,10,15–17] or electrotrophs for oxygen, CO_2, Cr(VI), chloramphenicol, nitrobenzene and nitrate reductions [11–14,18–22], to date, no essential attention has been paid to the MECs with biocathodes and driven by MFCs (Fig. 1) as a promising technology for simultaneous enhanced Cu(II) and Co(II) removal, and thus efficient Cu(II) and Co(II) wastewaters treatment.

A unique bacterial community is critical for the performance of biocathodes [11–14,18–22]. Under an applied voltage from MFCs with Cu(II) removal, biocathodes of the connected MECs are expected to be developed with an unique constitution of bacterial community for enhanced Co(II) removal inside, which may in turn improve Cu(II) removal in the MFCs. While initial Cu(II) concentration and ratio of electrode surface area and reactor volume greatly affected individual MFC performance [2,23–25], exploring effects of initial Cu(II) concentration and working volume in the cathode chambers of MFCs under a same cathode surface area is expected to enhance performance of MFCs and thus improve Cu(II) and Co(II) removal rates in this system.

In this study, the feasibility of MECs with biocathodes and driven by MFCs for simultaneous enhanced Co(II) and Cu(II) removal was explored. Kinetic parameters including initial Cu(II) concentration and working volume in the cathode chambers of MFCs were examined for enhanced Cu(II) and Co(II) removal. Cu(II) and Co(II) removal rates, anodic coulombic efficiencies (CEs) in MFCs and MECs, copper yield in the cathode chambers of MFCs, yields of cobalt, hydrogen, organics and biomass in the biocathode chambers of MECs, and overall system efficiency were extensively used to evaluate system performance. The diversity and composition of the bacterial community on the cathodes of MECs were characterized using high-throughput 16S rRNA gene sequencing.

2 Materials and methods

2.1 Reactor assembly

Two-chamber MFCs and MECs (duplicates) were used in

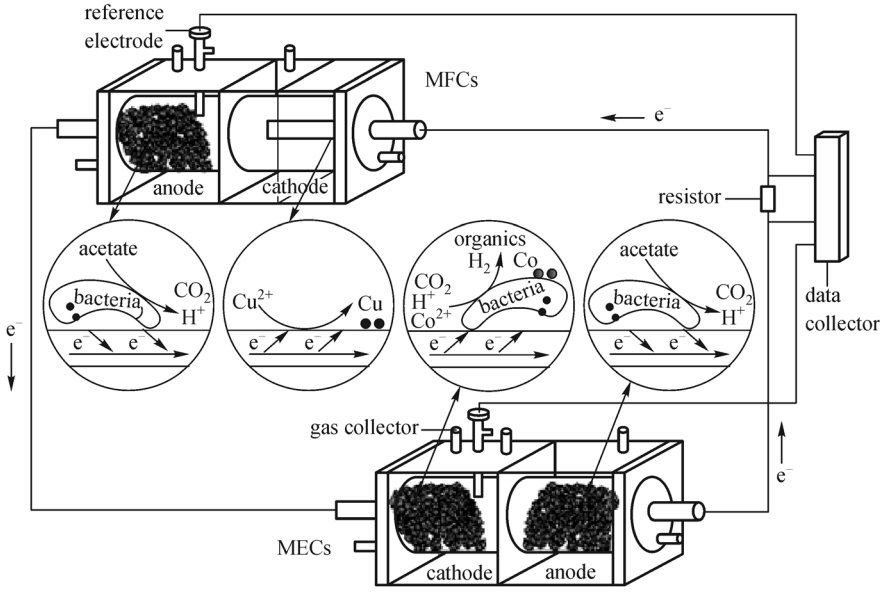

Fig. 1 Schematic diagram of MECs with biocathodes and driven by MFCs for simultaneous enhanced Cu(II) and Co(II) removal

all experiments, with the chambers separated by a cation exchange membrane (CEM) (CMI-7000 Membranes International, Glen Rock, NJ, USA). Graphite felt (Sanye Co., Beijing, China) was used as the anodes of MFCs and MECs with a working volume of 25 mL, respectively. Carbon rod (CR, Chijiu Duratight Carbon Co., Qingdao, China) with a projected surface area of 5.5 cm^2 was used as the cathodes of MFCs. Porous graphite felt (Sanye Co., Beijing, China) was served as the cathodes of MECs. For initial experiments, the working volumes in the cathode chambers of MFCs and MECs were 25 mL, respectively. These electrode materials were washed first in 32% HCl and then in 35% NaOH to remove metals from the surface.

2.2 Inoculation, acclimation and operation

The inoculation and acclimation procedures of MFCs and MECs were described in detail in Section S1.1 in Supplementary Material (SM). After 7 batch cycles and the potentials of anodes and cathodes in both MECs and MFCs were unchangeable, the MFCs and the MECs with biocathodes were regarded as individually well-developed and the finish of acclimation. The MFCs and MECs were then connected each other and stabilized for another 1–2 batch cycles before subsequent experiments. In tests of Cu (II) concentration, values of 5, 50, 500, and 1000 $mg \cdot L^{-1}$ were explored at an identical solution conductivity (SC) of 8.3 $mS \cdot cm^{-1}$ (adjusted by 0.1 $mol \cdot L^{-1}$ NaCl) while a Co (II) concentration of 40 $mg \cdot L^{-1}$ at a same SC of 8.3 $mS \cdot cm^{-1}$ (adjusted by 0.1 $mol \cdot L^{-1}$ NaCl) was always used in the cathode chambers of MECs. In the case of working volume in the cathode chambers of MFCs, system performance with a smaller volume of 13 mL was compared to that with the previous 25 mL under an identical cathode of carbon rod with the same surface area, similar to the reported description [9,23–25]. The reactor operation condition, open circuit controls (OCCs) and closed circuit controls (CCCs) were described in Section S1.1 in SM.

2.3 Measurements

Electrical data were collected using an automatic data acquisition system (PISO-813, Hongge Co., Taiwan, China). All potentials shown here were corrected to a SHE. Current density normalization was described in Section S1.2 in SM. The cathode redox behavior was studied using cyclic voltammetry (CV, CHI 650, Chenhua, Shanghai, China) at a scan rate of 1.0 $mV \cdot s^{-1}$. Linear sweep voltammetry (LSV) was performed using a potentiostat (CHI 650, Chenhua, Shanghai, China) at a scan rate of 0.1 $mV \cdot s^{-1}$. The three electrode system for both LSV and CV consisted of a working electrode (cathode electrode), counter electrode (platinum plate), and Ag/AgCl reference electrode (195 mV versus a SHE).

Species of Cu(II), Co(II), hydrogen, organics and biomass were determined according to the details (SM). Scanning electronic microscopy (SEM) (QUANTA450, FEI company, USA) equipped with an energy dispersive X-ray spectrometer (EDS) (X-MAX 20 $mm^2 \cdot 50\ mm^{-2}$, Oxford Instruments, UK) was used to examine the morphologies of both biocathodes of MECs and cathodes of MFCs, as well as elemental composition after the samples were necessarily vacuum-dried at 50°C overnight. The biocathodes of MECs needed to be specifically fixed overnight with 2% (v/v) paraformaldehyde and 2% (v/v) glutaraldehyde in 0.1 $mol \cdot L^{-1}$ cacodylate buffer (pH 7.5, 4°C), followed by washing and dehydration in water/ethanol solutions. Samples were then coated with Au/Pt before SEM observation.

2.4 Bacterial community analysis

Samples were collected from the biocathodes of MECs at the end of experiments with an initial Cu(II) concentration of 1000 $mg \cdot L^{-1}$ and a smaller working volume of 13 mL in the cathode chambers of MFCs. Since values of Cu(II) and Co(II) removal rates, and electrical data in the duplicate reactors were highly similar, bacterial communities in these reactors were presumably homologous each other. To acquire the compositions of bacterial communities reflecting the entire reactors, five pieces of graphite felt (1 cm × 1 cm × 1 cm) were removed from multiple locations on the electrodes in each of the duplicate reactors and mixed together for analysis. Bacterial community results from this sample thus reasonably reflected those in the duplicate reactors. The genomic DNA was extracted for quantitative and qualitative assessment, and purified with a DNA purification kit (Cat: SK8131, Sangon Biotech (Shanghai) Co. Ltd., China).

PCR reactions used universal 16S rRNA primers (Illumina Miseq). After the PCR amplification, the amplicons were recovered with gelose extraction kit (Cat: SK8131, Sangon Biotech (Shanghai) Co. Ltd., China) and rinsed with Tris-HCl solution. After amplication and quantified, the amplicons was used for sequencing analysis on an Illumina Miseq following the sequencing method manual. This analysis was performed in Sangon Biotech (Shanghai) Co. Ltd., China. The data were optimized through removing low-quality sequences, unrecognized reverse primer, with any ambiguous base calls, with a length < 300 bp.

2.5 Calculations

Cu(II) and Co(II) removal rates ($mg \cdot L^{-1} \cdot h^{-1}$) were calculated as the changes of Cu(II) and Co(II) concentrations divided by an operational period of 6 h, respectively, based on the multiple cycles of fed batch operation. An operation time of 6 h was used here mainly due to the removal of the majority of Cu(II) and Co(II) (71%–78%) at initial concentrations of 40–50 $mg \cdot L^{-1}$ and a working

volume of 25 mL in the cathode chambers of MFCs during this period. Anodic *CE*s in MFCs ($CE_{MFC,an}$, %) and MECs ($CE_{MEC,an}$, %), yields of copper (Y_{Cu}, $mol \cdot mol^{-1}$ COD), cobalt (Y_{Co}, $mol \cdot mol^{-1}$ COD), hydrogen (Y_{H_2}, $mol \cdot mol^{-1}$ COD), organics (Y_{org}, $mol \cdot mol^{-1}$ COD), and biomass (Y_{bio}, $mol \cdot mol^{-1}$ COD), and system efficiency (η_{sys}, %) were calculated according to Eqs. (1)–(8) (Section S1.3 in SM).

3 Results and discussion

3.1 Performance of MECs with biocathodes and driven by MFCs

A Cu(II) removal rate of $6.0 \pm 0.2\ mg \cdot L^{-1} \cdot h^{-1}$ was achieved at an initial concentration of $50\ mg \cdot L^{-1}$ in MFCs, compared to $1.2 \pm 0.1\ mg \cdot L^{-1} \cdot h^{-1}$ in the parallel OCCs (Fig. 2(a)), implying the importance of circuit current on Cu(II) removal. The Cu(II) removal in OCCs was mainly ascribed to chemical adsorption. This Cu(II) removal rate was 1.7 times as high as that in MECs with abiotic cathodes and driven by MFCs at similar solution and reactor conditions [9], demonstrating the positive effects of biocathode MECs on the connected MFCs for Cu (II) removal. An open circuit potential (OCP) of 0.68 V and a maximal power density of $4.8\ W \cdot m^{-3}$ ($21.9\ A \cdot m^{-3}$) were observed in MFCs (Fig. 2(b)). Concomitant with the occurrence in MFCs, Co(II) in the biocathode MECs was removed at a rate of $5.3 \pm 0.4\ mg \cdot L^{-1} \cdot h^{-1}$ and an initial concentration of $40\ mg \cdot L^{-1}$, apparently higher than $3.2 \pm 0.1\ mg \cdot L^{-1} \cdot h^{-1}$ in the biotic OCCs and 3.3 times of $1.6 \pm 0.1\ mg \cdot L^{-1} \cdot h^{-1}$ in the abiotic CCCs (Fig. 2(a)), demonstrating the importance of both circuit current and microorganisms on Co(II) removal in the MECs. Removal of Co(II) in the abiotic CCCs were mainly ascribed to chemical reduction and physical adsorption whereas observation in the biotic OCCs included processes associated with the presence of bacteria, such as bio-adsorption/bio-chelating in addition to physical adsorption, and biological reduction of Co(II). A Y_{Cu} of $0.24 \pm 0.01\ mol \cdot mol^{-1}$ COD was obtained in MFCs whereas Y_{Co} of $0.17 \pm 0.01\ mol \cdot mol^{-1}$ COD, Y_{org} of $0.10 \pm 0.00\ mol \cdot mol^{-1}$ COD and Y_{bio} of $0.08 \pm 0.00\ mol \cdot mol^{-1}$ COD were observed in the biocathode MECs (Table 1). Values of $CE_{MFC,an}$ and $CE_{MEC,an}$ reached 43%–55%, generally lower than those in single MFCs and MECs, mainly ascribed to the stacking connection and the consequent internal electron loss [17,26].

CV is a powerful technique for the study of the extracellular electron-transfer of electroactive microbial biofilm and useful thermodynamic and qualitative information on the electron transfer process can be also extracted from CV experiments. No redox peaks were observed in either the abiotic controls or biotic controls with the absence of Co(II) (Fig. 2(c)). One apparent reductive peak of −0.17 V appeared in the biofilm in the presence of Co(II), significantly more positive than −0.37 V observed in the abiotic controls. However, the peak current of −2.89 mA in the abiotic electrodes was higher than −1.33 mA in the biotic electrodes with the same presence of Co(II) (Fig. 2(c)). A more positive reductive potential on the biotic electrodes indicated a decrease in the overall free energy of the electron transfer reaction, mainly due to bacterial and bacterial component interactions with the electrode surface, which would decrease the energy required for Co(II) removal [27]. A lower reductive peak current on the biotic cathodes, however, suggested some degree of mass transfer inhibition due to the bacterial attachment to the electrode surface [27]. Other researchers also observed similar results, where biotic cathodes for hydrogen evolution and Au(III) or Co (II) recovery had lower reductive peak currents than abiotic cathodes despite the biotic cathodes having more positive potentials [27,28]. In addition, current density based on only the biofilm-covered area (which can only roughly estimated by microscopic examination) was recently suggested as a relatively good method for assessing BES performance, particularly for electrodes of porous graphite felt as used here [29]. Considering the generally sparse coverage of bacteria on the cathodes [18,19,21] and the presence of non-electrochemically active microbes in the mixed cultures, the actual current density based on electrochemically active biofilm-covered area was presumably higher than that of the abiotic controls, despite the somewhat higher reduction peak currents (in terms of mA) in the abiotic controls.

The scan rate is the speed of potential change per unit of time in a voltammetric experiment and it is the change of potential as function of time. The peak currents were examined at different scan rates (ν) ($1–10\ mV \cdot s^{-1}$) to determine the rate limiting step [30,31]. When a plot of the peak current versus ν is linear, the results indicate "thin-film behavior", and therefore that electron transfer from the electrode to the bacteria is slower than intracellular reactions. If the peak is current proportional to $\nu^{1/2}$, this indicates a diffusion-controlled regime [30,31]. The current was not limited by diffusion and showed a linear dependency to the scan rate (Fig. 2(d)), previously proved to be a typical thin film behavior [30]. This suggested that the biofilm might allow solute diffusion through biofilm to a relatively greater extent than biofilm containing dense extracellular matrix did. The gradients of scans under biotic conditions were steeper than that in abiotic controls, indicating a change in the kinetic behavior of the electron transfer reaction, which was probably a rate-limiting step in BESs in many cases.

3.2 Electrode morphologies and product analysis

SEM images clearly showed distinctive structure and morphology (Fig. 3). The cathode surface in MFCs was

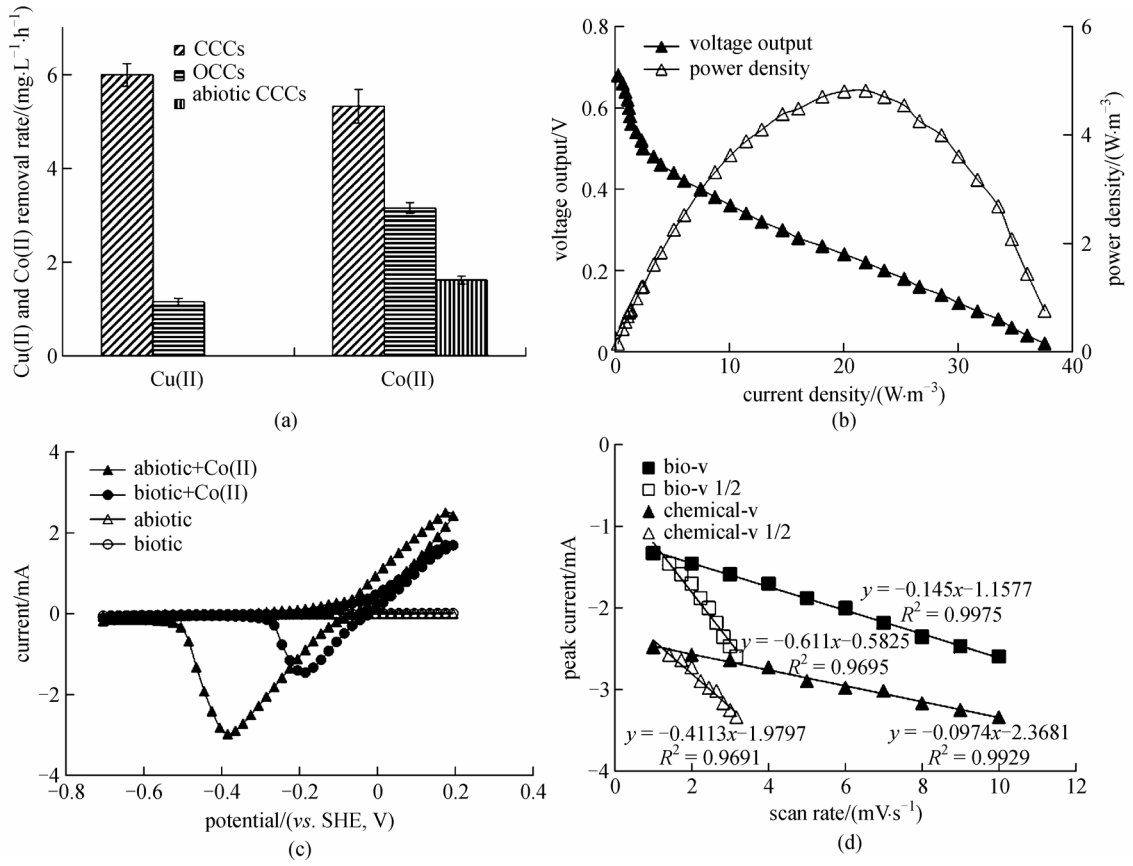

Fig. 2 (a) Cu(II) and Co(II) removal rates, (b) polarization curve of MFCs, (c) cyclic voltammetry tests on the biocathodes of MECs, and (d) peak current – scan rate on the biotic and abiotic cathodes of MECs (working volume in the cathode chambers of MFCs: 25 mL)

Table 1 Yields of copper, cobalt, hydrogen, organics and biomass, and operational efficiencies in the MECs with biocathodes and driven by MFCs under various conditions

working volume /mL	initial Cu(II) concentration /(mg·L^{-1})	*CE*		η_{sys}/%	yield				
		$CE_{MFC,an}$ /%	$CE_{MEC,an}$ /%		Y_{Cu} /(mol·mol^{-1} COD)	Y_{Co} /(mol·mol^{-1} COD)	Y_{H_2} /(mol·mol^{-1} COD)	Y_{org} /(mol·mol^{-1} COD)	Y_{bio} /(mol·mol^{-1} COD)
25	5	43.3±0.2	47.3±0.2	6.2±0.1	0.06±0.00	0.19±0.00	—	0.07±0.00	0.07±0.00
	50	45.5±0.1	53.9±0.1	10.4±0.4	0.24±0.01	0.17±0.01	—	0.10±0.00	0.08±0.00
	500	51.4±0.7	54.2±0.7	33.6±0.8	1.21±0.04	0.10±0.00	0.01±0.00	0.03±0.00	0.04±0.00
	1000	55.1±0.2	54.7±0.2	42.0±0.2	1.61±0.00	0.08±0.00	0.02±0.00	0.02±0.00	0.01±0.00
13	1000	58.0±0.1	60.0±0.2	51.4±0.1	1.95±0.60	0.07±0.00	0.05±0.00	0.01±0.00	0.01±0.00

uniformly covered by a polycrystalline face centered cubic structure on a micrometer scale after Cu(II) removal (Fig. 3 (a)). Using EDS to examine the composition of the precipitates on the cathodes of MFCs, Cu signals were observed (Fig. 3(c)). The ratio of Cu and O was approximate 7, much higher than the 2 as a final product of Cu_2O, implying most Cu(II) was reduced to pure copper [2]. On the surfaces of the cathodes of MECs, however, the biofilm was composed of cells with a relatively homogeneous morphology (Fig. 3(b)), consistent with the reported thinner biofilm corresponded with better biocathode performance [18,19,21,22]. The determination of Co signals located on bacterial surface and the absence of Co signals on the electrodes with no bacteria covered (Fig. S2 in SM) implied that Co(II) removal was associated with bacteria (Fig. 3(d)). Compared to the electrodes with no

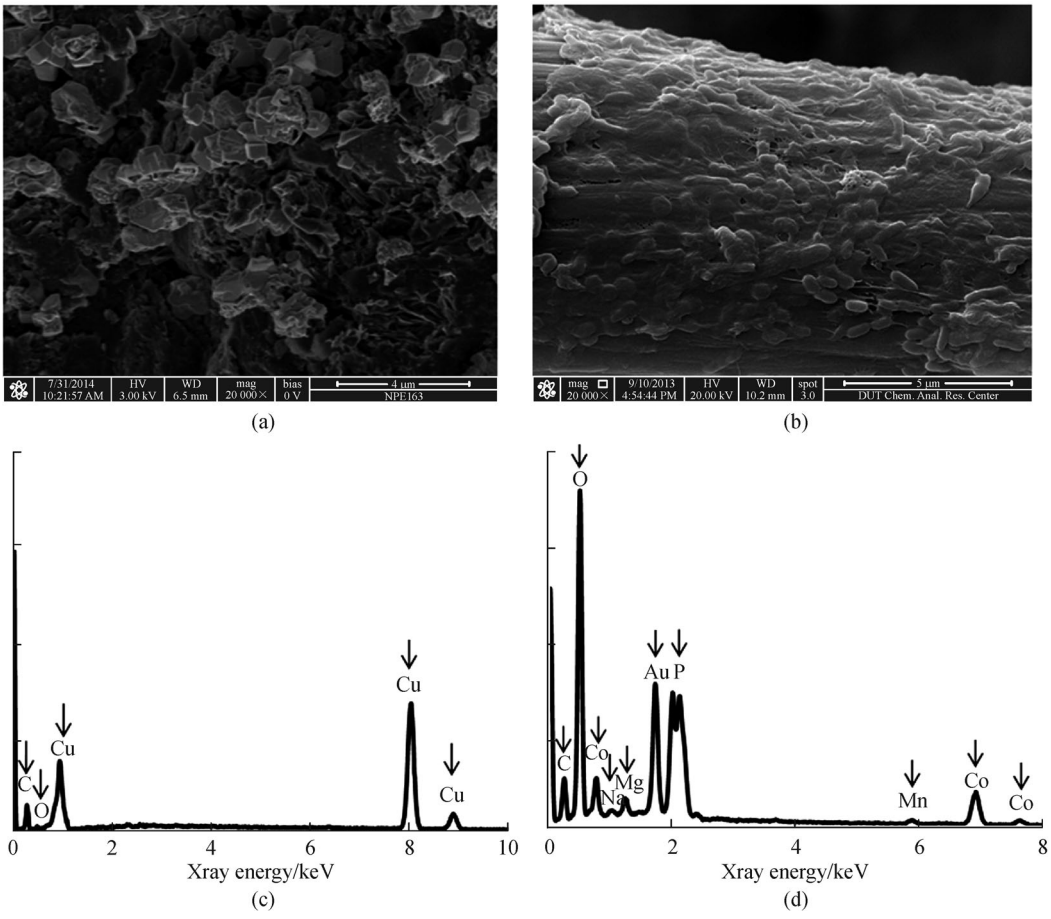

Fig. 3 SEM observation on the cathodes of (a) MFCs and (b) MECs after around 10 fed-batch cycles operation (square indicates the location of EDS analysis). EDS results on products of (c) Cu(II) reduction and (d) Co(II) removal associated with bacteria

bacteria covered, higher amount of C and O together with other multiple elements including Na, Mg, P and Mn was observed on the bacteria covered electrodes, mainly ascribed to the composition of bacterial cells. The appearance of Au signals on the electrodes with and without bacteria covered was associated with sample pretreatment.

The products formed on the cathodes mainly depend on substrate concentration and pH value. Under the present experimental condition, cathode theoretical potentials at different pHs were calculated based on the Nernst equations (Fig. 4). Considering the final pHs of 2.8–2.9 in the cathode chambers of MFCs and 5.4–5.6 in the biocathode chambers of MECs, Cu(II) and Co(II) were presumably changed to Cu(0) (Fig. 4(a)) and Co(0) (Fig. 4 (b)), respectively despite that Co(II) may be additionally chelated on the cellular surface. Cu(0) and Co(0) crystals can be also attributable to the cathodic environment which was strictly sustained to a minimal initial dissolved oxygen below 0.7 $mg \cdot L^{-1}$. Under an aerobic/facultative environment, dissolved oxygen can compete with species of Cu(II) and phenols for cathodic provided electrons, resulting in the formation of partial reduction products [2,32].

3.3 System performance with increased initial Cu(II) concentrations

Both Cu(II) and Co(II) removal rates increased with the increase in initial Cu(II) concentration, from 1.0±0.0 $mg \cdot L^{-1} \cdot h^{-1}$ for Cu(II) (Fig. 5(a)) and 4.4±0.1 $mg \cdot L^{-1} \cdot h^{-1}$ for Co(II) (Fig. 5(b)) at an initial Cu(II) of 5 $mg \cdot L^{-1}$ to 82.6±0.2 $mg \cdot L^{-1} \cdot h^{-1}$ (Cu(II)) (Fig. 5(a)) and 6.0±0.2 $mg \cdot L^{-1} \cdot h^{-1}$ (Co(II)) (Fig. 5(b)) at a Cu(II) of 1000 $mg \cdot L^{-1}$. Accordingly, Y_{Cu}, Y_{H2} and η_{sys} exhibited similar trends, achieving the maximal 1.61±0.00 $mol \cdot mol^{-1}$ COD, 0.02±0.00 $mol \cdot mol^{-1}$ COD and 42.0±0.2%, respectively at the highest Cu(II) of 1000 $mg \cdot L^{-1}$ (Table 1).

An increase in Cu(II) concentration from 50 $mg \cdot L^{-1}$ to 1000 $mg \cdot L^{-1}$ had less effects on OCP but substantially improved power density from 4.8 $W \cdot m^{-3}$ to 26 $W \cdot m^{-3}$ (Fig. 5(c)). A much low initial Cu(II) of 5 $mg \cdot L^{-1}$ resulted in a low OCP of 0.6 V and a low power density of 2.2 $W \cdot m^{-3}$. While a high Cu(II) was beneficial for $CE_{MFC,an}$ and $CE_{MEC,an}$ (Table 1), an increase in Cu(II) concentration reasonably improved voltages applied in the connected MECs and thus resulted in the subsequent more negative potentials of the biocathodes (Fig. 5(d)). Both of them

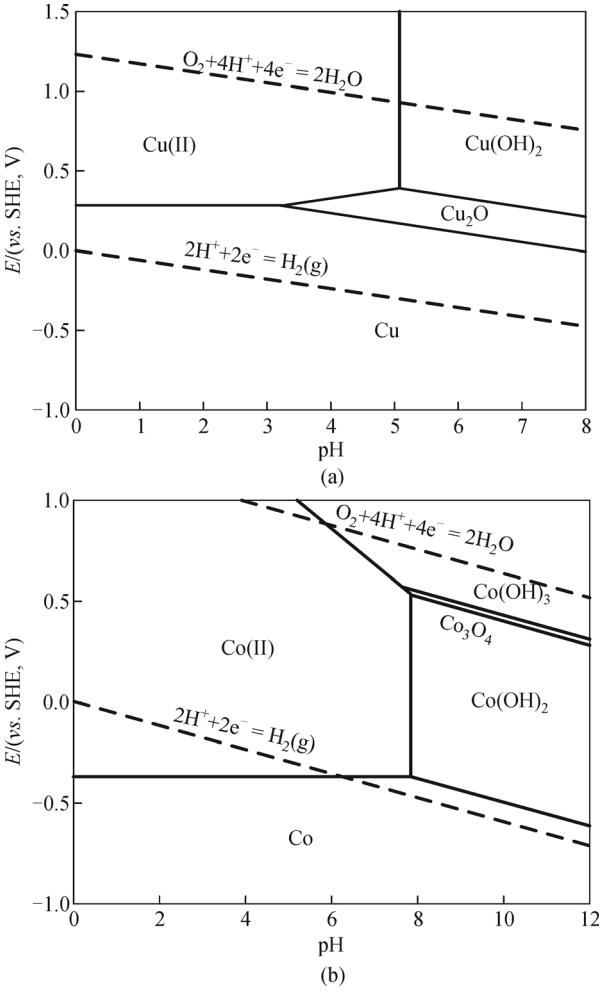

Fig. 4 Theoretical cathode potentials for half-reactions of (a) Cu (II) to Cu(I), Cu(II) to Cu and Cu(I) to Cu, and (b) Co(III) to Co(II), Co(III) to Co_3O_4 and Co(II) to Co, at different pH values

explained the more efficient Co(II) removal in the biocathodes of MECs (Fig. 5(b)). Higher applied voltages in the MECs at higher Cu(II) concentrations had extracted more electrons from organics in the anodes of MECs and led to subsequent more COD consumption, explaining the lower Y_{Co} at a higher Cu(II) concentration (Table 1).

CV analysis clearly showed the shift of reductive peaks on the cathodes of MFCs to higher potentials with the increase in initial Cu(II) concentration (Fig. 5(e)), implying the positive effects of high Cu(II) concentrations on electrochemical reduction. The appearance of multiple reductive peaks particular at higher Cu(II) concentrations of 500 $mg \cdot L^{-1}$ and 1000 $mg \cdot L^{-1}$ was mainly ascribed to the multiple reaction intermediates possibly occurred for the final product of pure copper (Fig. 4(a)). LSV (Fig. 5(f)) indicated that at a high Cu(II) concentration of 1000 $mg \cdot L^{-1}$, the reduction current increased rapidly until reaching a peak current of $-11.6\ A \cdot m^{-2}$ at a potential of -0.40 V, where the reaction was limited by the copper ion transfer. With the decrease in Cu(II) concentration, cathodic reaction rate decreased and reached a similar current density of $-0.09\ A \cdot m^{-2}$ at -0.02 V for Cu(II) at 5 $mg \cdot L^{-1}$ and 50 $mg \cdot L^{-1}$. This current density was referred to as mass transfer limitation polarization current.

3.4 System performance with smaller working volumes in the cathode chambers of MFCs

A smaller working volume of 13 mL in the cathode chambers of MFCs was tested here for enhanced Cu(II) and Co(II) removal rates in this system. A Cu(II) removal rate of 115.7±0.8 $mg \cdot L^{-1} \cdot h^{-1}$ (Fig. 6(a)) with a Y_{Cu} of 1.95±0.60 $mol \cdot mol^{-1}$ COD (Table 1) was achieved in MFCs, much higher than the 82.6±0.2 $mg \cdot L^{-1} \cdot h^{-1}$ and 1.61±0.00 $mol \cdot mol^{-1}$ COD with 25 mL (Fig. 5(a) and Table 1). Accordingly, an OCP of 0.73 V and a maximal power density of 27 $W \cdot m^{-3}$ (87 $A \cdot m^{-3}$) were obtained from MFCs with 13 mL (Fig. 6(b)), higher than the 0.70 V and 26 $W \cdot m^{-3}$ (76 $A \cdot m^{-3}$) at 25 mL (Fig. 5(c)), mainly ascribed to the decrease in internal resistance (Fig. 6(a)) and demonstrating the preferable small working volumes in the cathode chambers of MFCs for high power production [9,23–25]. The efficient MFCs reasonably resulted in increased applied voltages and more negative potentials of the biocathodes in MECs (Fig. 6(c)), as well as higher circuit currents (Fig. 6(d)). All of them may have been beneficial for Co(II) removal and hydrogen generation, leading to a Co(II) removal rate of 6.4±0.2 $mg \cdot L^{-1} \cdot h^{-1}$ (Fig. 6(a)) and a hydrogen yield of 0.05±0.00 $mol \cdot mol^{-1}$ COD (Table 1). Both of them were higher than the 6.0±0.2 $mg \cdot L^{-1} \cdot h^{-1}$ and 0.02±0.00 $mol \cdot mol^{-1}$ COD with 25 mL (Fig. 5(b) and Table 1). These results illustrated the importance of enhanced MFCs with smaller working volumes in the cathode chambers for improved Co(II) removal and hydrogen generation in the connected MECs. However, similar values of Y_{Co} were obtained with 13 mL and 25 mL (Table 1). This result was mainly ascribed to an equivalent increase in COD consumption in the anodes and Co(II) decrease in the cathodes of the same MECs due to the decreased volume of 13 mL in the cathode chambers of MFCs (Eq. (4) in Section 1.3 in SM).

These Cu(II) and Co(II) removal rates could not be compared with conventional electrochemical processes due to greatly different operational conditions and reactor architectures [1]. However, energy consumption in conventional electrochemical processes for cobalt and copper recovery amounted to 3.9–28.3 $kWh \cdot kg^{-1}$ Co at more acidic pHs 3.0–4.0 and a higher temperature of 50°C [1] and 102 $kWh \cdot kg^{-1}$ Cu at a more acidic pH of 1.0 [33], compared to zero energy consumption here, reflecting the energy-saving merit of this system. Moreover, Cu(II) removal rate here was 3.4–38 times of individual MFCs at a similar Cu(II) concentration of 800–1000 $mg \cdot L^{-1}$ but with various reactor architectures [2,34] whereas the Co(II)

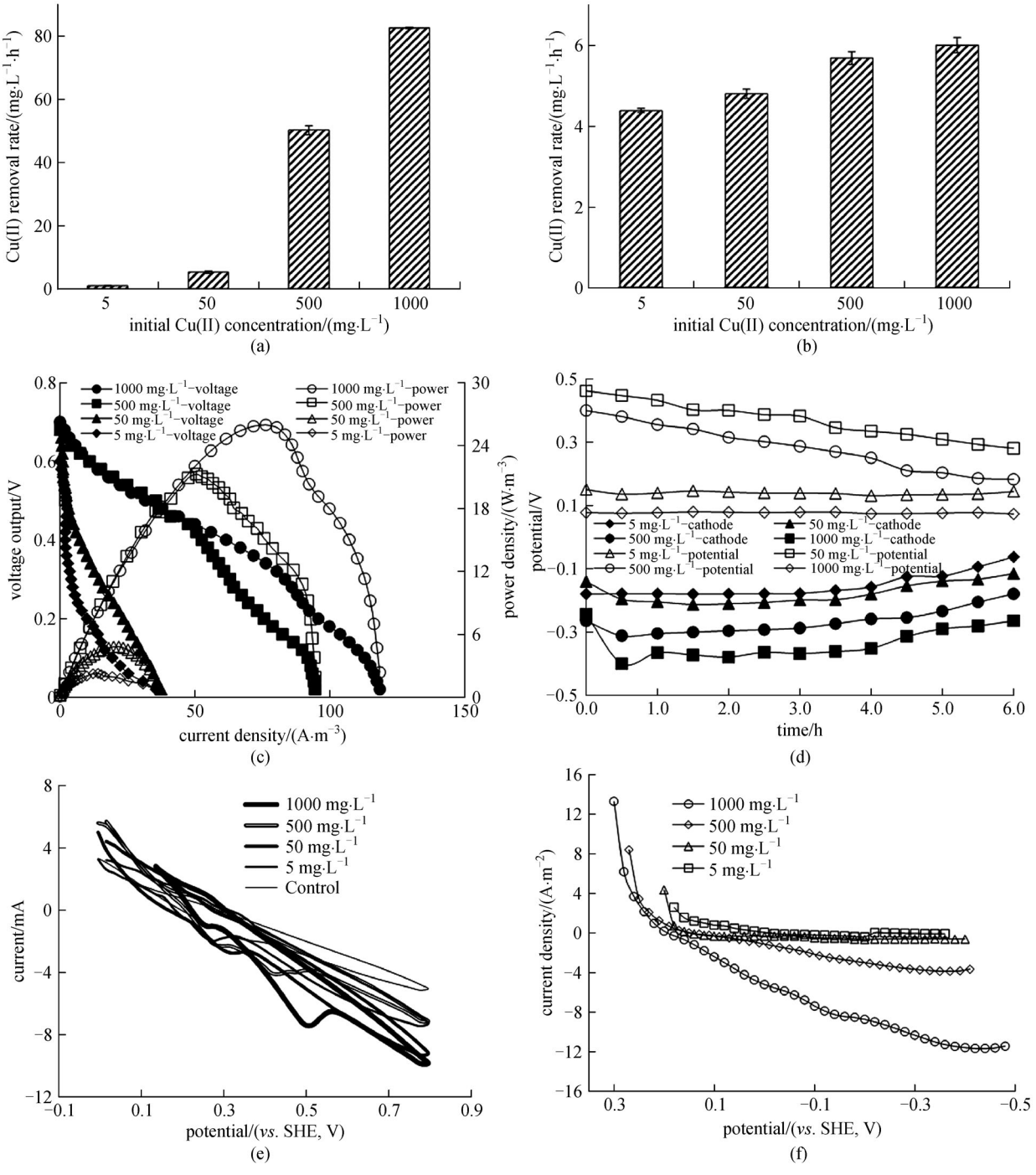

Fig. 5 (a) Cu(II) and (b) Co(II) removal rates, (c) polarization curve of MFCs, (d) applied voltage and cathode potential in the biocathode MECs, (e) cyclic voltammetry tests and (f) linear sweep voltammetry on the cathodes of MFCs under various initial Cu(II) concentration conditions (working volume in the cathode chambers of MFCs: 25 mL)

removal rate was 2.2 times of individual MECs with biocathodes at similar solution conditions with requirement of an additional energy consumption of 1.6 kWh·kg^{-1} Co [3]. Compared to the MECs with abiotic cathodes and driven by MFCs under similar solution and reactor conditions [9], Co(II) and Cu(II) removal rates here were 3.3 times and 1.7 times as high as those in the former, demonstrating the more efficiency of the present systems for Cu(II) and Co(II) removals. In a total consideration, MECs with biocathodes and driven by MFCs provides an alternative strategy for simultaneous enhanced copper and cobalt recovery without any external energy consumption.

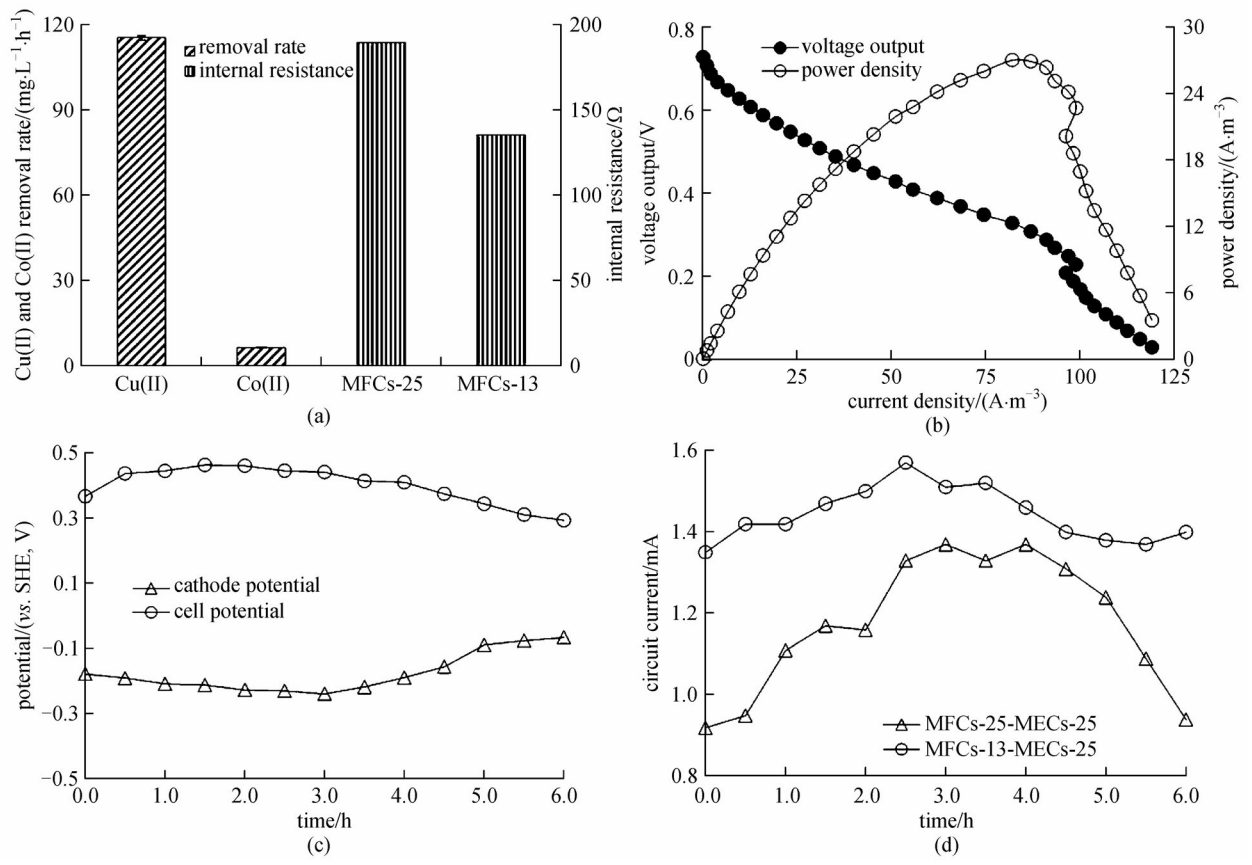

Fig. 6 (a) Cu(II) and Co(II) removal rates, and internal resistances of MFCs, (b) polarization curves of MFCs, (c) applied voltage and cathode potential, and (d) circuit current in the biocathode MECs under a smaller working volume of 13 mL in the cathode chambers of MFCs (initial Cu(II) concentration: 1000 mg·L^{-1})

3.5 Bacterial community structure of cathode biofilm

The qualified sequences of 28118 with an average length of 412 nucleotides were obtained from the biofilm on the cathode. The sequences were clustered to represent operational taxonomic units (OTUs) with 0.03 distances. The core bacterial OTUs were defined as the OTUs greater than 0.5% of the total sequence reads. The total OTUs observed for biofilm were 1316. Shannon index was 4.78 and Chao1 richness estimator yielded total OTUs of 2563.

Phylogenetic analysis indicated that populations fell into 6 phyla, among which the absolute majority of sequences belonged to *Proteobacteria* and accounted for 67.9% of the total reads in the biofilm (Fig. 7(a)). This agreed with the previous study in cobalt-rich deep-sea sediment [35]. Other major bacterial phyla included *Firmicutes* (14.0%), *Bacteroidetes* (6.1%), *Tenericutes* (2.5%), *Lentisphaerae* (1.4%), *Synergistetes* (1.0%), and other 8 minor phyla (0.7%). Despite the ubiquitous majority of these phyla in BESs, the phyla *Firmicutes* and *Bacteroidetes* were more abundant than those in conventional cobalt-rich sites [35], implying the providence of a good environment for these phyla. Besides the classified phyla, 6.5% of the total reads was unclassified on the phylum level.

Class level classification of the biofilm indicated 12 predominant bacterial classes, which in total contributed to 92.7% of the entire reads (Fig. 7(b)). *Proteobacteria* was comprised of α- (33.7%), β- (23.8%), γ- (9.0%), and δ- (1.2%) classes. The bacterial community composition based on family and genus levels were shown in Figs. S3 and S4 in SM.

While many genera within the biofilm had functional roles that remained unknown, the function of some genera in this community has been known to be associated with heavy metal resistance/removal or electrotrophic/exoelectrogenic characters, and thus may have played important roles in the present biocathodes of MECs. There was no exactly positive correlation between the dominant microorganisms and either electrotrophic activities or Co(II) removal. A small group of microbes may have played a numerically dominant role in this process. In addition, interspecies cooperation cannot be excluded in order to forward the diverse processes of Co(II) removal, hydrogen evolution, bacterial growth and extracellular organics synthesis. The electrotrophic activities in these chemolithotrophic processes still remain unknown. The microorganisms found here may own some specific characters relating with Co(II) removal, hydrogen evolution, extra-

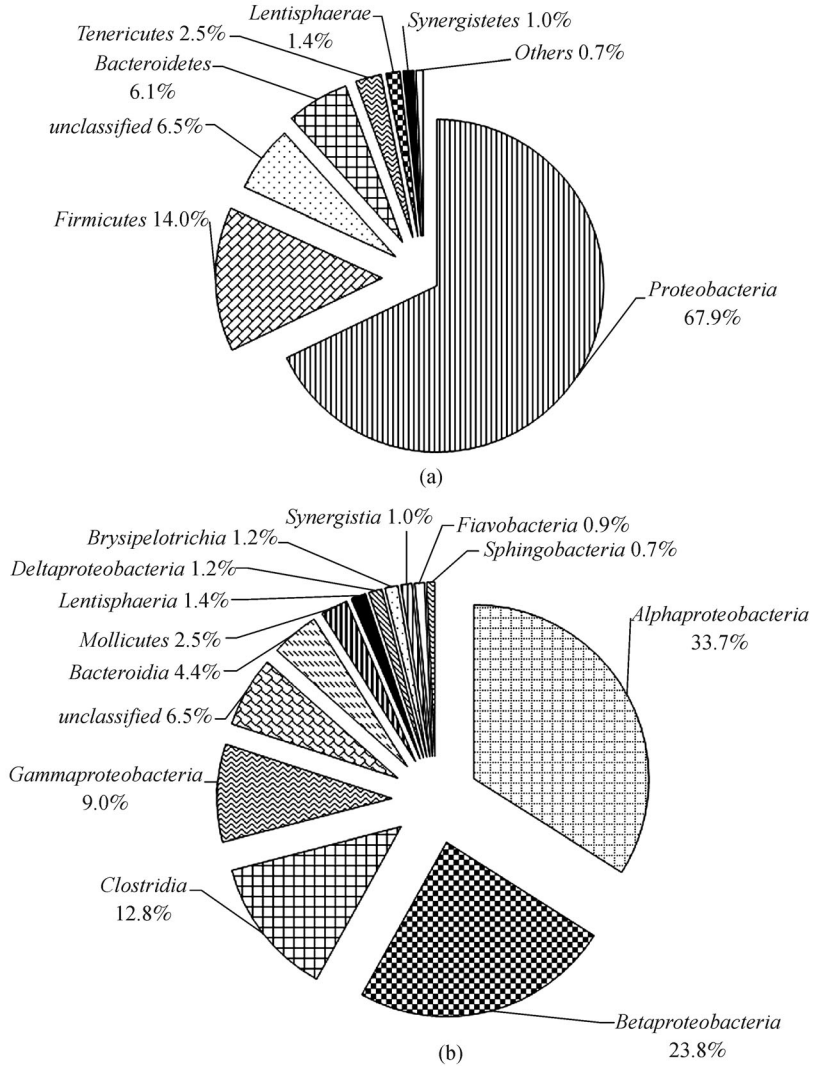

Fig. 7 Relative abundance of bacterial reads retrieved from the biocathodes of MECs classified at the (a) phylum and (b) class level. Phyla and classes that represented less than 0.5% of the total bacterial community composition were classified as "*others*"

cellular organics synthesis and electrotrophic activities. Further investigations in these directions based on pure cultures are warranted.

4 Outlook

This study was the first attempt at applying MFCs to drive MECs with biocathodes for simultaneous enhanced Cu(II) and Co(II) removal without any external energy consumption. This process can be considered a proper approach as it is not modified by the direct addition of any substrate. Such a process of no external energy input also brings us closer to a zero-emission and zero-energy consumption target. This in-site utilization of electricity from MFCs may also provide more environmental benefits compared to direct harvest electricity from MFCs [4].

The MECs with biocathodes and driven by MFCs will not displace existing methods of electrochemical or chemical-physical processes, especially for high-strength Cu(II) and Co(II) recovery. Instead, this system will likely be more appropriate for treatment of relatively dilute effluents containing Co(II) and Cu(II) ions. The process herein described has also some other limitations. As an example, proper separation of the recovered cobalt from the microorganisms and the recovered copper from the cathodes should be further carried out in order to achieve a fully copper and cobalt recycling process. In view of the co-present Cu(II) and Co(II) in the effluents of spent lithium ion battery treatment processes [1] as well as the merit of Co(II) removal in MECs instead of MFCs, an influent of mixed Cu(II) and Co(II) is previously suggested to be initially fed into the cathode chambers of MFCs for Cu(II) reduction and the effluent of the cathodes of MFCs

is then employed in the cathode chambers of MECs for Co (II) removal [9,10]. Since the predictable detrimental effects of Cu(II) ions and more acidic pHs on the cathodic biofilm in the present MECs, an appropriate Cu(II) concentration in the mixed influent with proper pHs (e.g. 5.0–7.0) is appreciably required to achieve a complete Cu (II) reduction on the cathodes of MFCs and thus avoids the adverse effects of Cu(II) and more acidic pHs on the electrotrophic activities in the connected MECs. In addition and in terms of product purity, the formation of pure copper on the cathodes of MFCs is heavily dependent on an anaerobic environment [2,31,32] whereas cobalt deposited on the biocathodes of MECs may have somewhat been chelating with the cellular surface and thus heavily depends on the characteristics of specific bacteria [3]. Relationship between the bacterial community and the specific mechanism cannot be concluded based on the species level results reported here. These will require product-directed specific bacteria screening and system performance optimization together with long-term operation assessment. Further investigations in these directions are strongly warranted.

5 Conclusions

Enhanced removal rates of $6.0\pm0.2\ mg\cdot L^{-1}\cdot h^{-1}$ for Cu(II) and $5.3\pm0.4\ mg\cdot L^{-1}\cdot h^{-1}$ for Co(II) were achieved in the system of MECs with biocathodes and driven by MFCs, 1.7 times and 3.3 times as high as those in the MECs with abiotic cathodes and driven by MFCs. A higher initial Cu (II) concentration of $1000\ mg\cdot L^{-1}$ and a smaller working volume of 13 mL in the cathode chambers of MFCs further improved Cu(II) and Co(II) removal rates, reaching 115.7 $mg\cdot L^{-1}\cdot h^{-1}$ and $6.4\ mg\cdot L^{-1}\cdot h^{-1}$, respectively with concomitantly achieving hydrogen generation of $0.05\pm0.00\ mol\cdot mol^{-1}$ COD. Phylogenetic analysis on the biocathodes illustrates *Proteobacteria* dominantly accounted for 67.9% of the total reads, followed by *Firmicutes* (14.0%), *Bacteroidetes* (6.1%), *Tenericutes* (2.5%), *Lentisphaerae* (1.4%) and *Synergistetes* (1.0%). This is the first reported investigation on MECs with biocathodes and driven by MFCs and provides a beneficial attempt for simultaneous enhanced copper and cobalt recovery, and efficient Cu(II) and Co(II) wastewaters treatment without any external energy consumption.

Acknowledgements The authors gratefully acknowledge financial support from the National Natural Science Foundation of China (Grant Nos. 51178077 and 21377019), Specialized Research Fund for the Doctoral Program of Higher Education "SRFDP" (No. 20120041110026) and Program for Changjiang Scholars and Innovative Research Team in University (IRT_13R05).

Supplementary material is available in the online version of this article at http://dx.doi.org/10.1007/s11783-015-0805-y and is accessible for authorized users.

References

1. Freitas M B J G, Celante V G, Pietre M K. Electrochemical recovery of cobalt and copper from spent Li-ion batteries as multilayer deposits. Journal of Power Sources, 2010, 195(10): 3309–3315
2. Tao H C, Liang M, Li W, Zhang L J, Ni J R, Wu W M. Removal of copper from aqueous solution by electrodeposition in cathode chamber of microbial fuel cell. Journal of Hazardous Materials, 2011, 189(1–2): 186–192
3. Jiang L, Huang L, Sun Y. Recovery of flakey cobalt from aqueous Co(II) with simultaneous hydrogen production in microbial electrolysis cells. International Journal of Hydrogen Energy, 2014, 39(2): 654–663
4. Li W, Yu H, He Z. Towards sustainable wastewater treatment by using microbial fuel cells-centered technologies. Energy & Environmental Science, 2014, 7(3): 911–924
5. Modin O, Wang X, Wu X, Rauch S, Fedje K K. Bioelectrochemical recovery of Cu, Pb, Cd, and Zn from dilute solutions. Journal of Hazardous Materials, 2012, 235–236: 291–297
6. Tao H C, Lei T, Shi G, Sun X N, Wei X Y, Zhang L J, Wu W M. Removal of heavy metals from fly ash leachate using combined bioelectrochemical systems and electrolysis. Journal of Hazardous Materials, 2014, 264: 1–7
7. Luo H, Liu G, Zhang R, Bai Y, Fu S, Hou Y. Heavy metal recovery combined with H_2 production from artificial acid mine drainage using the microbial electrolysis cell. Journal of Hazardous Materials, 2014, 270: 153–159
8. Luo H, Qin B, Liu G, Zhang R, Tang Y, Hou Y. Selective recovery of Cu^{2+} and Ni^{2+} from wastewater using bioelectrochemical system. Frontiers of Environmental Science & Engineering, 2015, 9 (3): 522–527.
9. Wu D, Pan Y, Huang L, Quan X, Yang J. Comparison of Co(II) reduction on three different cathodes of microbial electrolysis cells driven by Cu(II)-reduced microbial fuel cells under various cathode volume conditions. Chemical Engineering Journal, 2015, 266: 121–132
10. Wu D, Pan Y, Huang L, Zhou P, Quan X, Chen H. Complete separation of Cu(II), Co(II) and Li(I) using self-driven MFCs-MECs with stainless steel mesh cathodes under continuous flow conditions. Separation and Purification Technology, 2015, 147: 114–124
11. Rosenbaum M A, Franks A E. Microbial catalysis in bioelectrochemical technologies: status quo, challenges and perspectives. Applied Microbiology and Biotechnology, 2014, 98(2): 509–518
12. Wang A, Cheng H, Ren N, Cui D, Lin N, Wu W. Sediment microbial fuel cell with floating biocathode for organic removal and energy recovery. Frontiers of Environmental Science & Engineering, 2012, 6(4): 569–574
13. Xia X, Sun Y, Liang P, Huang X. Long-term effect of set potential on biocathodes in microbial fuel cells: electrochemical and phylogenetic characterization. Bioresource Technology, 2012, 120: 26–33
14. Huang L, Regan J M, Quan X. Electron transfer mechanisms, new applications, and performance of biocathode microbial fuel cells. Bioresource Technology, 2011, 102(1): 316–323
15. Wang Y, Liu X, Li W, Li F, Wang Y, Sheng G, Zeng R, Yu H. A

microbial fuel cell-membrane bioreactor integrated system for cost-effective wastewater treatment. Applied Energy, 2012, 98: 230–235

16. Fradler K R, Michie I, Dinsdale R M, Guwy A J, Premier G C. Augmenting microbial fuel cell power by coupling with supported liquid membrane permeation for zinc recovery. Water Research, 2014, 55: 115–125
17. Huang L, Yao B, Wu D, Quan X. Complete cobalt recovery from lithium cobalt oxide in self-driven microbial fuel cell-microbial electrolysis cell systems. Journal of Power Sources, 2014, 259: 54–64
18. Huang L, Chai X, Chen G, Logan B E. Effect of set potential on hexavalent chromium reduction and electricity generation from biocathode microbial fuel cells. Environmental Science & Technology, 2011, 45(11): 5025–5031
19. Wang A J, Cheng H Y, Liang B, Ren N Q, Cui D, Lin N, Kim B H, Rabaey K. Efficient reduction of nitrobenzene to aniline with a biocatalyzed cathode. Environmental Science & Technology, 2011, 45(23): 10186–10193
20. Zhang G, Zhao Q, Jiao Y, Zhang J, Jiang J, Ren N, Kim B H. Improved performance of microbial fuel cell using combination biocathode of graphite fiber brush and graphite granules. Journal of Power Sources, 2011, 196(15): 6036–6041
21. Huang L, Chai X, Quan X, Logan B E, Chen G. Reductive dechlorination and mineralization of pentachlorophenol in biocathode microbial fuel cells. Bioresource Technology, 2012, 111: 167–174
22. Liang P, Wei J, Li M, Huang X. Scaling up a novel denitrifying microbial fuel cell with an oxic-anoxic two stage biocathode. Frontiers of Environmental Science & Engineering, 2013, 7(6): 913–919
23. Fan Y, Hu H, Liu H. Enhanced Coulombic efficiency and power density of air-cathode microbial fuel cells with an improved cell configuration. Journal of Power Sources, 2007, 171(2): 348–354
24. Fan Y, Han S K, Liu H. Improved performance of CEA microbial fuel cells with increased reactor size. Energy & Environmental Science, 2012, 5(8): 8273–8280
25. Logan B E. Essential data and techniques for conducting microbial fuel cell and other types of bioelectrochemical system experiments. ChemSusChem, 2012, 5(6): 988–994
26. Zhang Y, Yu L, Wu D, Huang L, Zhou P, Quan X, Chen G. Dependency of simultaneous Cr(VI), Cu(II) and Cd(II) reduction on the cathodes of microbial electrolysis cells self-driven by microbial fuel cells. Journal of Power Sources, 2015, 273: 1103–1113
27. Varia J, Martínez S S, Orta S V, Bull S, Roy S. Bioelectrochemical metal remediation and recovery of Au^{3+}, Co^{2+} and Fe^{3+} metal ions. Electrochimica Acta, 2013, 95: 125–131
28. Batlle-Vilanova P, Puig S, Gonzalez-Olmos R, Vilajeliu-Pons A, Bañeras L, Balaguer M D, Colprim J. Assessment of biotic and abiotic graphite cathodes for hydrogen production in microbial electrolysis cells. International Journal of Hydrogen Energy, 2014, 39(3): 1297–1305
29. Sharma M, Bajracharya S, Gildemyn S, Patil S A, Alvarez-Gallego Y, Pant D, Rabaey K, Dominguez-Benetton X. A critical revisit of the key parameters used to describe microbial electrochemical systems. Electrochimica Acta, 2014, 140: 191–208
30. Harnisch F, Freguia S. A basic tutorial on cyclic voltammetry for the investigation of electroactive microbial biofilms. Chemistry, an Asian Journal, 2012, 7(3): 466–475
31. Huang L, Liu Y, Yu L, Quan X, Chen G. A new clean approach for production of cobalt dihydroxide from aqueous Co(II) using oxygen-reducing biocathode microbial fuel cells. Journal of Cleaner Production, 2015, 86: 441–446
32. Huang L, Shi Y, Wang N, Dong Y. Anaerobic/aerobic conditions and biostimulation for enhanced chlorophenols degradation in biocathode microbial fuel cells. Biodegradation, 2014, 25(4): 615–632
33. Silva-Martínez S, Roy S. Copper recovery from tin stripping solution: Galvanostatic deposition in a batch-recycle system. Separation and Purification Technology, 2013, 118: 6–12
34. Cheng S A, Wang B S, Wang Y H. Increasing efficiencies of microbial fuel cells for collaborative treatment of copper and organic wastewater by designing reactor and selecting operating parameters. Bioresource Technology, 2013, 147: 332–337
35. Liao L, Xu X W, Jiang X W, Wang C S, Zhang D S, Ni J Y, Wu M. Microbial diversity in deep-sea sediment from the cobalt-rich crust deposit region in the Pacific Ocean. FEMS Microbiology Ecology, 2011, 78(3): 565–585